Inactivation of Single Cardiac Na^+ Channels in Three Different Gating Modes

Thomas Böhle,*# Matthias Steinbis,* Christoph Biskup,* Rolf Koopmann,* and Klaus Benndorf*
*Department of Physiology, Friedrich-Schiller-University, D-07740 Jena, and #Department of Physiology, University of Cologne, D-50931 Cologne, Germany

ABSTRACT In small cell-attached patches containing one and only one Na^+ channel, inactivation was studied in three different gating modes, namely, the fast-inactivating F mode and the more slowly inactivating S mode and P mode with similar inactivation kinetics. In each of these modes, ensemble-averaged currents could be fitted with a Hodgkin-Huxley-type model with a single exponential for inactivation (τ_h). τ_h declined from 1.0 ms at −60 mV to 0.1 ms at 0 mV in the F mode, from 4.6 ms at −40 mV to 1.1 ms at 0 mV in the S mode, and from 4.5 ms at −40 mV to 0.8 ms at +20 mV in the P mode, respectively. The probability of non-empty traces (*net*), the mean number of openings per non-empty trace (*op/tr*), and the mean open probability per trace (p_{open}) were evaluated at 4-ms test pulses. *net* inclined from 30% at −60 mV to 63% at 0 mV in the F mode, from 4% at −90 mV to 90% at 0 mV in the S mode, and from 2% at −60 mV to 79% at +20 mV in the P mode. *op/tr* declined from 1.4 at −60 mV to 1.1 at 0 mV in the F mode, from 4.0 at −60 mV to 1.2 at 0 mV in the S mode, and from 2.9 at −40 mV to 1.6 at +20 mV in the P mode. p_{open} was bell-shaped with a maximum of 5% at −30 mV in the F mode, 48% at −50 mV in the S mode, and 16% at 0 mV in the P mode. It is concluded that 1) a switch between F and S modes may reflect a functional change of inactivation, 2) a switch between S and P modes may reflect a functional change of activation, 3) τ_h is mainly determined by the latency until the first channel opening in the F mode and by the number of reopenings in the S and P modes, 4) at least in the S and P modes, inactivation is independent of pore opening, and 5) in the S mode, mainly open channels inactivate, and in the P mode, mainly closed channels inactivate.

INTRODUCTION

In cardiac Na^+ channels, the decay of macroscopic current consists of at least two kinetic components (Zilberter and Motin, 1991; Mitsuiye and Noma, 1995; Grant and Starmer, 1987; Saint et al., 1992), with characteristic time constants of inactivation (τ_{h1} and τ_{h2}). Generally, it is assumed that each time constant represents a transition into a distinct inactivated state. These transitions are thought (Correa and Bezanilla, 1994) to be either coupled (one inactivated state has to be passed to reach the next one) or independent (each inactivated state is reached directly either from an open or a non-inactivated closed state). From results of both single-channel experiments (Patlak and Ortiz, 1985) and whole-cell recordings (Chandler and Meves, 1970; Gilly and Armstrong, 1984; Attwell et al., 1979; Keynes and Meves, 1993; Keynes, 1994), the existence of at least two different gating modes of Na^+-channel action has been postulated, which mainly differ in inactivation kinetics. By using a low-noise recording technique (Benndorf, 1993, 1995), we recently unraveled five distinct gating modes of Na^+-channel action (Böhle and Benndorf, 1995a,b), which differ in activation and/or inactivation kinetics. The modes have a characteristic pattern of voltage dependence of mean open-channel lifetime (τ_o), time before which one-half of the first channel openings have occurred ($t_{0.5}$), and steady-state activation. The lifetime of the modes, determined from the long-time course of the averaged current per trace, is variable, being in the range of some seconds (lower border of identification) to several minutes. With respect to inactivation kinetics, the modes were named as the fast-inactivating (F), the intermediate 1 (M1), the intermediate 2 (M2), the slow (S), and the persistent (P) mode. In this study, we focus on inactivation properties of the F, S, and P modes. We exclude the M1 and the M2 mode, because our present data are insufficient. In the meanwhile, it turned out that the P mode also inactivates; i.e., it is not persistent. To avoid confusion, however, the term P mode will be continued to be used. In the present report, the dependence of inactivation on the test-pulse voltage is investigated by the analysis of the time constant of macroscopic inactivation (τ_h), the probability of non-empty traces (*net*), the mean number of openings per non-empty trace (*op/tr*), and the mean open probability per trace (p_{open}). These data, in combination with results from previously published experiments, are interpreted with respect to functional changes in channel gating that may cause mode switching.

Received for publication 21 November 1997 and in final form 29 June 1998.

Address reprint requests to Dr. Thomas Böhle, Department of Physiology, Friedrich-Schiller-University, Teichgraben 8, D-07740 Jena, Germany. Tel.: 49-3641-934350; Fax: 49-3641-933202; E-mail: boehle@mti-n.uni-jena.de.

0006-3495/98/10/1740/09 $2.00

MATERIALS AND METHODS

Cell preparation, temperature, and solutions

Single cells of heart ventricles from adult white mice were isolated according to the procedure described by Benndorf (1993). The experiments were performed at 23 ± 1°C in a bath solution that contained (in mM) 230 KCl, 20 CsCl, 1 $MgCl_2$, 10 EGTA, 5 HEPES, pH 7.3, and a pipette solution

that contained (in mM) 255 NaCl, 2.5 $CaCl_2$, 4 KCl, 5 HEPES, pH 7.3. The elevated Na^+ concentration was used to enhance unitary current amplitudes (Yue et al., 1989).

Patch pipettes and pipette holders

For the purpose of low-noise recording (Benndorf, 1993), patch pipettes were prepared from thick-walled borosilicate-glass tubing (Hilgenberg, Malsfeld, Germany) with an external diameter of 2.0 mm and an internal diameter of 0.5 mm or 0.25 mm. The patch pipettes were inserted into a pipette holder of small dimension manufactured from polycarbonate (Benndorf, 1993) or into an improved version consisting completely of silver (Benndorf, 1995). Pipette tips were generated only seconds before starting gigaohm seal formation by breaking off the final tip region at the glass bottom of the bath chamber (Böhle and Benndorf, 1994). Gigaohm seals were obtained after touching the cell membrane by application of slight suction.

Data acquisition and analysis

Unitary Na^+-channel currents were recorded at a sampling rate of 66 or 100 kHz in the cell-attached patch configuration with an Axopatch-200A amplifier (integrating headstage, intrinsic noise, 0.059 pA rms at 5 kHz; Axon Instruments, Foster City, CA). Analog filtering was performed with an eight-pole Bessel filter at a band width of 20 kHz (48 dB/octave; Frequency Devices, Inc., Haverhill, MA). When data needed further filtering for the analysis, an off-line Gaussian-filter algorithm was used. If not otherwise noted, the holding potential was −120 mV. Duration of prepulses was 20 ms, and 4-ms pulses were applied at a rate of 5–20 Hz. In part of the experiments, the various pulse potentials were applied alternately. The mode-specific and voltage-dependent open probability was constant. Capacitive transients were compensated for carefully via compensation circuits containing in summary four exponentials. Leakage and remaining capacitive currents were removed by subtracting averaged blank traces, which were formed exclusively from traces in the neighborhood of the actual sweep. None of the patches in the present study showed any sign of containing more than one active Na^+ channel. This was verified by inspecting several thousands of consecutive traces at pulses to −40 mV or more positive potentials to exclude the existence of any superimposition of opening events. For curve fitting, a derivative-free Levenberg-Marquardt routine (Brown and Dennis, 1972) was used. Recording and analysis were performed on a PC-80486 or PC-Pentium with the ISO2-software (MFK-Computer, Niedernhausen, Germany).

Gating modes were at first selected by the average-of-interval plots. Those parts of these data plots suspected to comprise one gating mode were investigated in further detail to unequivocally define the respective gating mode. This has been described extensively in Böhle and Benndorf (1995a). The final criteria for identification of gating modes are both the mean open time and the first latency. All data were checked for the combination of these two criteria before further investigation. Only after this procedure was the inactivation time constant (τ_h) determined. Subsequently, the probability of non-empty traces (*net*), the mean number of openings per non-empty trace (*op/tr*), and the mean open probability per trace (p_{open}) were analyzed.

RESULTS

Fig. 1 *A* shows the long-time course of an experiment, in which an alteration of the gating mode appeared. In these average-of-interval plots (cf. Böhle and Benndorf, 1995a,b), each dot represents the averaged current of an individual trace of 4 ms duration at −40 mV. During the time interval of ~70 s in the left, the Na^+ channel was gating in the F mode, and during the time interval of ~55 s in the right, the same channel was gating in the P mode. The gating mode has changed at the same pulse protocol. During the time interval of 18 min between both recordings, the Na^+ channel was gating in multiple modes with lifetimes being too short to identify them. In Fig. 1 *B*, 16 consecutive individual traces of the respective recordings in Fig. 1 *A* are presented. In the F mode, the Na^+ channel opens shortly only once or

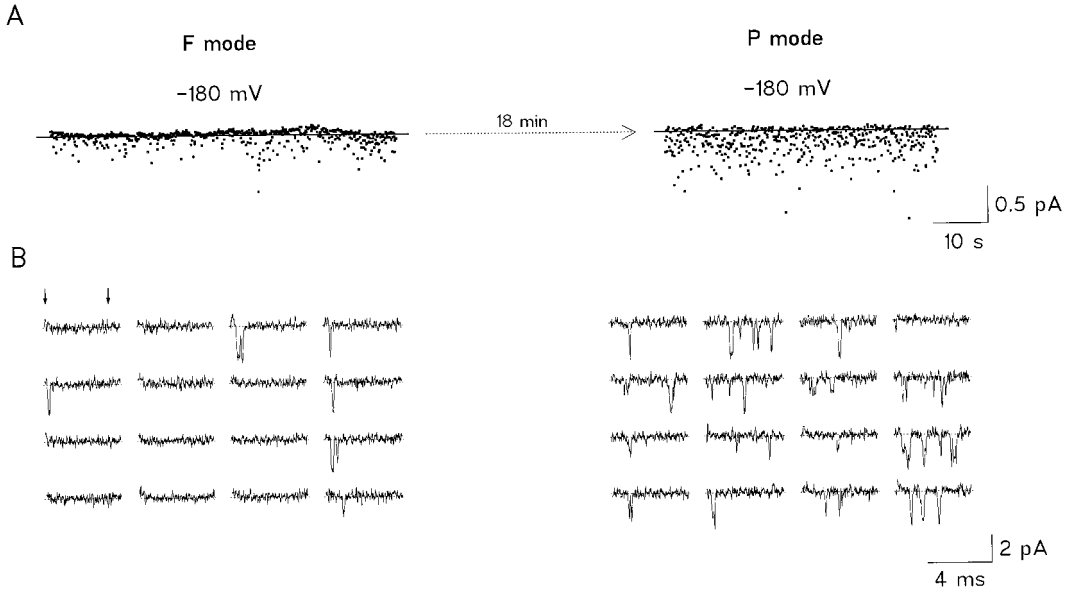

FIGURE 1 Alteration of the gating mode (F to P mode transition) at the same pulse protocol. (*A*) Plots of the long-time course of the averaged current per trace (the zero-current level is at the dotted horizontal arrow; 640 traces in the F mode, *left*; 501 traces in the P mode, *right*; 4-ms depolarizations to −40 mV after 20-ms prepulses to −180 mV; filter, 20 kHz). (*B*) Sixteen consecutive single-channel current traces from *A* in the F mode (*left*) and in the P mode (*right*), respectively. The vertical arrows indicate beginning and end of the test pulses (filter, 5 kHz).

twice directly after the pulse beginning. In the P mode, the duration of openings is very similar to that in the F mode, but reopenings may occur during the whole pulse. In contrast to the F mode, first latency is long in the P mode (Böhle and Benndorf, 1995a,b).

Long-time recording from another Na^+ channel is illustrated in Fig. 2 *A*. Fast and reversible switchings between different plateaus are prominent in the average-of-interval plots. We previously showed (Böhle and Benndorf, 1995a,b) that the plateau-like patterns formed by the distribution of dots in the average-of-interval plots may be used as a rough measure for the identification of gating modes, which may be precisely identified only by the additional analysis of the mean open time and the first latency. In the time intervals of Fig. 2, the Na^+ channel was gating either in the P mode (plateau of small amplitude) or the S mode (plateau of large amplitude). In the left and in the middle, 20-ms prepulses to −180 mV and in the right to −70 mV were applied. Sudden back or forth switching appeared both at hyperpolarized and depolarized prepulse potentials. In Fig. 2 *B*, eight consecutive single-channel current traces directly before and after each mode switching are illustrated. Again, in the P mode, first latency is slow, openings are short, and reopenings may occur during the whole pulse. Heterogeneous levels in current amplitude may be caused by unresolved fast flickering. In the S mode, openings start promptly after the pulse beginning and last occasionally over the whole pulse duration. In the fourth column from the right, the arrow points to an opening in the S mode that had appeared at the prepulse to −70 mV.

Fig. 3 shows ensemble-averaged currents in single-channel patches at test pulses to −40 and 0 mV in the F, S, and P modes, respectively. Gating modes were identified by average-of-interval plots and the analysis of open-channel lifetime and first latency. Macroscopic kinetics of Na^+ current are characteristic in each mode. In the F mode, fast activation is followed by fast inactivation; in the S mode, fast activation is followed by slow inactivation; and in the P mode, slow activation is followed by slow inactivation. The mode-specific kinetics of the currents were fitted with a Hodgkin-Huxley model of the type Am^3h. The magnitude of the parameters amplitude (A), activation time constant (τ_m), and inactivation time constant (τ_h) is indicated for each mode. The kinetics of activation in the F and S modes are not fully resolved at both potentials, but the data show that in the P mode, τ_m is slower by a factor of ~2. Comparison of the first latency yields a respective factor of ~5 (Böhle and Benndorf, 1995b). More accurate comparison is possible for τ_h. In the S and P modes, the inactivation time constant is largely the same and more than 10 times slower compared with the F mode. Within each mode, τ_h is faster at 0 mV than at −40 mV by a factor of ~4. The voltage dependence of τ_h in the three modes is illustrated in Fig. 4 in greater detail. In both the S and P modes, reasonable Hodgkin-Huxley fits were obtained only at −40 mV and more positive potentials. In these two modes, τ_h is indistinguishable. In the F mode, Hodgkin-Huxley fits yielded substantially lower τ_h values. The degree of voltage dependence of τ_h is similar in the three modes.

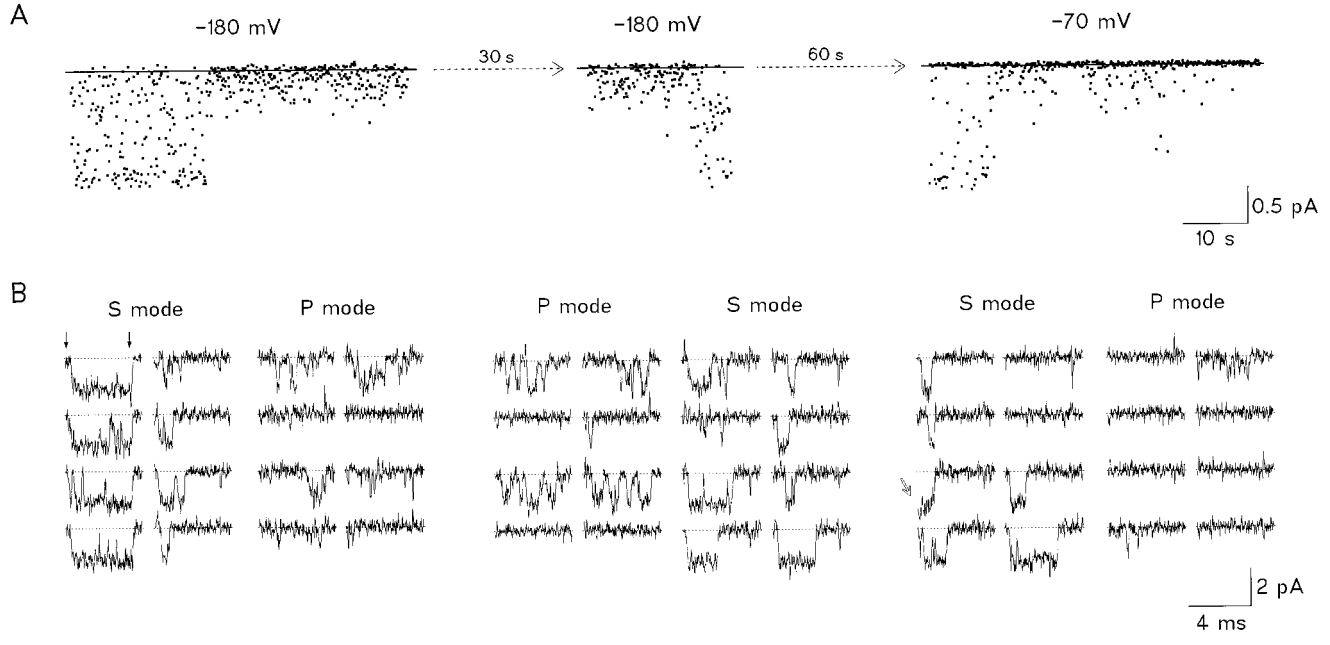

FIGURE 2 Sudden back and forth switching between different gating modes (S mode and P mode) after hyperpolarized as well as after depolarized prepulse potentials. (*A*) Plots of the long-time course of the averaged current per trace (filter, 20 kHz) at 4-ms depolarizations to −40 mV after 20-ms prepulses to −180 mV (508 and 504 traces, *left* and *middle*, respectively) and −70 mV (495 traces, *right*). (*B*) Single-channel current traces from *A* directly before and after switching between the S mode and the P mode (filter, 5 kHz). The vertical arrows indicate beginning and end of the test pulses. The small inclined arrow at the third trace from above in the fourth column from the right points to a channel opening in the S mode that had arisen at the prepulse to −70 mV.

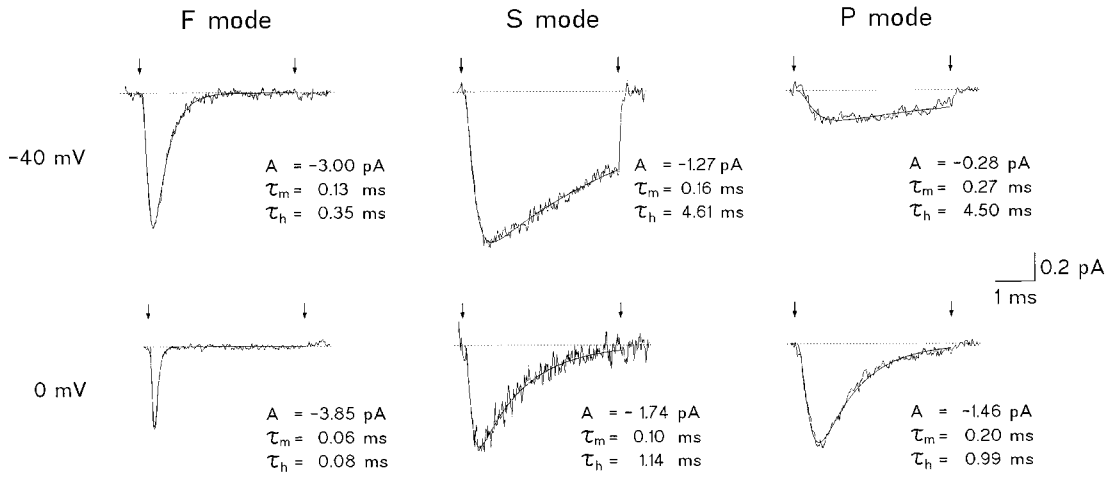

FIGURE 3 Hodgkin-Huxley fit (Am^3h) of ensemble-averaged currents at −40 mV and 0 mV in the F, S, and P modes, respectively (the parameters A, τ_m, and τ_h are indicated; the included trace numbers are F mode, 544 at −40 mV, 401 at 0 mV; S mode, 496 at −40 mV, 109 at 0 mV; P mode, 501 at −40 mV, 500 at 0 mV; the vertical arrows indicate beginning and end of the test pulses; filter, 5 kHz).

To learn more about inactivation in each mode, we analyzed the probability of non-empty traces (*net*), the mean number of openings per non-empty trace (*op/tr*), and the mean open probability per trace (p_{open}). For determination of opening and closing, a split threshold procedure (60% and 40% of the mean open level; cf Fig. 5) was used. The mean open level was determined from amplitude histograms that were formed by eliminating the transition points with the variance-mean technique as introduced by Patlak (1988). In the upper part of the figure, the idealized trace computed from the original trace in the lower part is illustrated.

The distribution of the number of openings per trace at test pulses to −40 and 0 mV is shown in Fig. 6. The mean number of openings per non-empty trace (*op/tr*), the probability of non-empty traces (*net*), and the mean open probability per trace (p_{open}; empty and non-empty traces) are indicated in each diagram. Two results should be pointed out. 1) At −40 mV, *op/tr* in the S and P modes is larger than in the F mode. 2) At 0 mV, p_{open} is much larger in the S and P modes than in the F mode.

Fig. 7 compares the voltage dependence of the probability of non-empty traces (*net*(*V*)) in the F, S, and P modes. In each mode, *net* increases at stronger depolarization. The lines connect data points from the same patch. The data show that due to different steady-state activation (Böhle and Benndorf, 1995b) in the S mode, *net* increases at less depolarized potentials than in both the F and P modes. Furthermore, *net*(*V*) in the F and P modes is similar despite notable differences in steady-state activation. A possible reason for this apparent contradiction is faster closed-channel inactivation in the F mode (see Discussion).

The respective voltage dependence of the mean number of openings per non-empty trace ((op/tr)(V)) is illustrated in

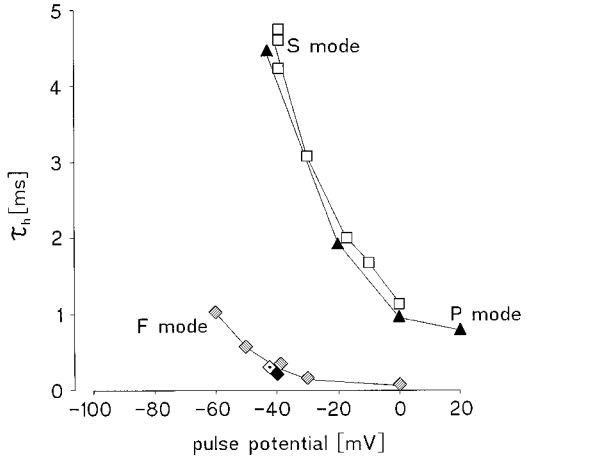

FIGURE 4 Voltage dependence of the inactivation time constant (τ_h) in the F, S, and P modes. For each mode, the same type of symbol was chosen, and equal filling of the symbols indicates the same patch. The symbols match with those in Figs. 7 and 8.

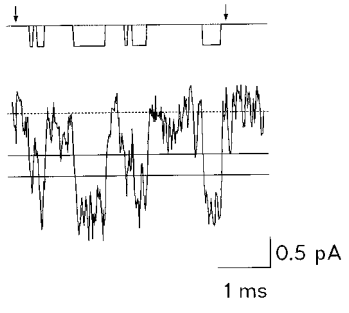

FIGURE 5 Method for determination of the probability of non-empty traces (*net*), the mean number of openings per non-empty trace (*op/tr*; this hence refers only to traces with openings), and the mean open probability per trace (p_{open}; empty and non-empty traces) with a split threshold for detection of opening and closing. The arrows indicate beginning and end of the test pulses. The upper trace is the idealized trace computed from the lower original trace (filter, 5 kHz).

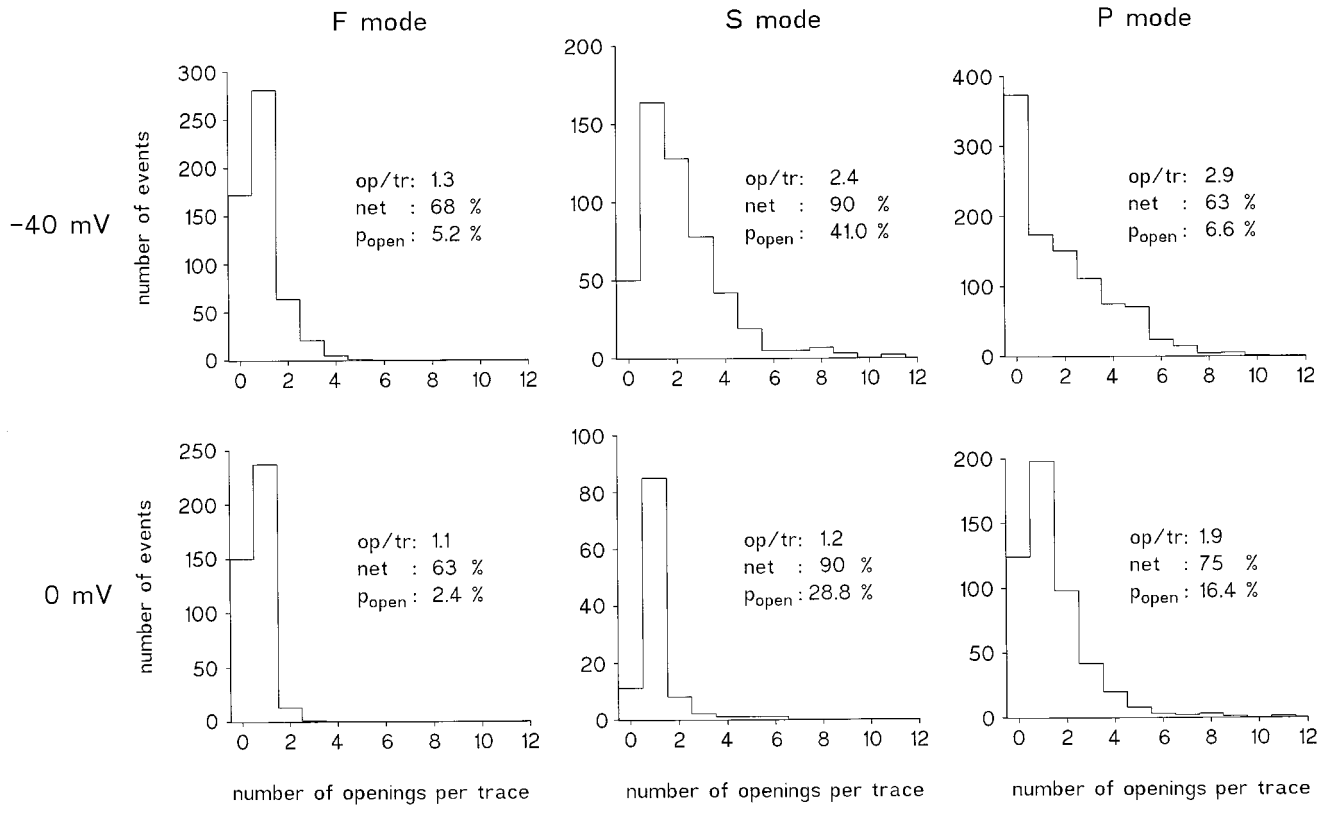

FIGURE 6 Distribution of the number of openings per trace at −40 mV and 0 mV in the F, S, and P modes, respectively. The probability of non-empty traces (*net*), the mean number of openings per non-empty trace (*op/tr*), and the mean open-probability per trace (p_{open}) is indicated (split threshold: opening level 87% and closing level 14.5% in the S mode at 0 mV; opening level 60% and closing level 40% in all other cases; filter, 5 kHz).

Fig. 8. Again, lines connect data points from single patches. In general, in the S and P modes, the 4-ms pulses were too short for complete inactivation. Therefore, the calculated mean number of openings per trace is an underestimation of the mean number of openings before inactivation. The stippled lines indicate voltage ranges in which activation interferes. In the voltage range where *op/tr* declines with depolarization, the S and P modes show a steeper voltage dependence than the F mode. In the S and P modes, the voltage dependence would be even steeper if one had mea-

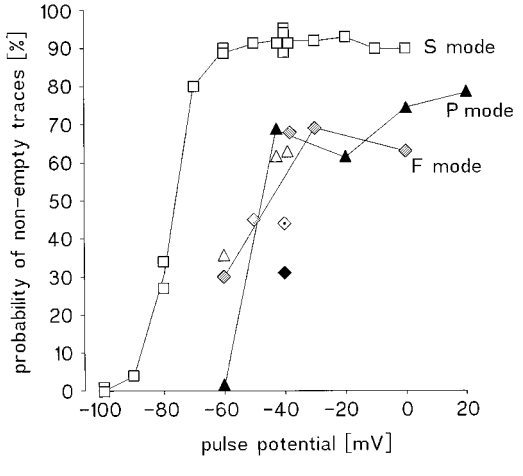

FIGURE 7 Voltage dependence of the probability of non-empty traces (*net*(*V*)) in the F, S, and P modes. Each line connects data points from a single patch (split threshold: opening level 70.6% and closing level 30.6% in the S mode at −10 mV; opening level 87% and closing level 14.5% in the S mode at 0 mV; opening level 60% and closing level 40% in all other cases; filter, 5 kHz).

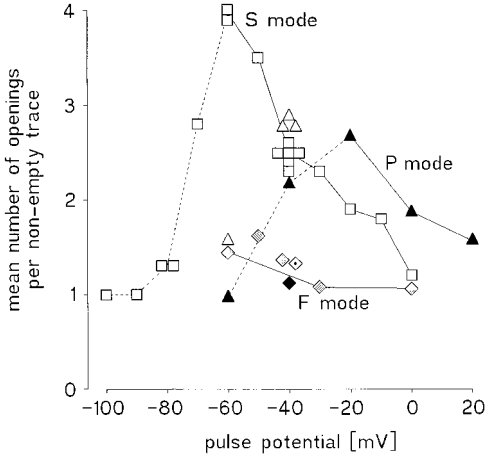

FIGURE 8 Voltage dependence of the mean number of openings per non-empty trace ((op/tr(V)) in the F, S, and P modes. Each line connects data points from a single patch (split threshold: same levels as given in legend to Fig. 5; filter, 5 kHz).

sured the actual mean number of openings before inactivation. In these modes, inactivation is incomplete at the end of the pulse, and this effect is more pronounced at the more negative voltages compared with the more positive voltages.

In Fig. 9, the voltage dependence of the mean open probability per trace ($p_{open}(V)$) is shown. A bell-shaped voltage dependence is observed in all three modes. $p_{open}(V)$ reaches a peak at −50 mV in the S mode, at −40 mV in the F mode, and at 0 mV in the P mode. With respect to the previous results, p_{open} is given by the product of *net*, *op/tr*, and the mean open time (τ_o) divided by the pulse duration. Thus p_{open} data depend strongly on the pulse duration. Attention should be paid to the enormous magnitude of p_{open} in the S mode. Only a few channels gating in the S mode would severely alter the electrical performance of a heart cell (see Discussion).

DISCUSSION

Functional relationship between modes

In patches containing a single Na^+ channel, we investigated three distinct gating modes (F mode, S mode, and P mode), which appeared randomly during the recording. We did not find any evidence that switching between the modes depended on the prepulse voltage. On the other hand, our data are not sufficient to exclude a possible voltage dependence in the occurrence of individual gating modes. Four voltage-dependent parameters associated with inactivation were determined: 1) the time constant of macroscopic inactivation ($\tau_h(V)$), 2) the probability of non-empty traces (*net*(V)), 3) the mean number of openings per non-empty trace (*op/tr*(V)), and 4) the mean open probability per trace ($p_{open}(V)$).

The most striking relationship between the modes are the similarity of activation kinetics and first latency (Böhle and Benndorf, 1995b) in the F and S modes and the similarity of inactivation kinetics in the S and P modes. These results suggest that a switching between the F and S modes is caused by a functional change in the inactivation process, whereas a switching between the S and P modes is caused by a functional change in the activation process. F and P modes differ by both activation and inactivation. The striking similarity of inactivation kinetics in the S and P modes is surprising, in particular when the differences in $p_{open}(V)$ are considered. Taken together, these two observations lead to the conclusion that in these two modes, the inactivation process is independent of the pore opening.

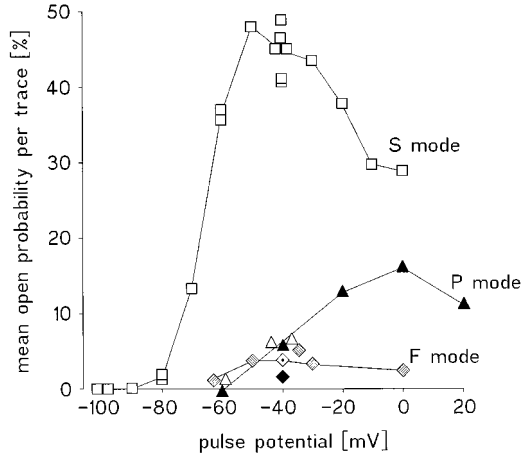

FIGURE 9 Voltage dependence of the mean open-probability per trace ($p_{open}(V)$) in the F, S, and P modes (split threshold: same levels as given in legend to Fig. 5; filter, 5 kHz).

Fig. 10 shows a model for the interdependence between the different gating modes. The F and S modes are assumed to have equal rate constants for activation ($\alpha_{F,S}$) and deactivation ($\beta_{F,S}$), which, however, differ from those in the P mode (α_P, β_P). The S and P modes are assumed to have equal rate constants for open- and closed-channel inactivation ($\delta_{S,P}$), which in turn are different from open- and closed-channel inactivation in the F mode (δ_F, γ_F). Recovery from inactivation is not taken into consideration because, at present, we have no data allowing any conclusion. At this point, it should be emphasized that a model implying the reductions mentioned must be an oversimplification. Nevertheless, this model seems to be useful for a general discussion.

Comparison of steady-state activation in the three modes (Böhle and Benndorf, 1995b) suggests also a similarity in the activation process of the F and S modes. Steady-state activation of the F and S modes seems to be similar when compared with that of the P mode, which is positioned at more depolarized voltages. The slight difference between F and S modes might be explained by faster closed-channel inactivation in the F mode.

In the F mode, inactivation from closed and open states is ascribed to different rate constants (δ_F,γ_F). If gating between the closed and the open state within the available system is assumed to be similar in the F and S modes, then there must be significant open-channel inactivation in the F mode (large δ_F). This conclusion results from the shorter mean open time in the F mode compared with that in the S mode. In our model, the openings in the F mode are shortened compared with those in the S mode because of faster open-channel inactivation. This interpretation is also supported by the rare appearance of reopenings in the F mode.

With regard to closed-channel inactivation in the F mode, (γ_F), our data do not allow any reliable conclusion. A parameter that should depend on closed-channel inactivation is the number of non-empty traces (*net*). In comparison with 90% *net* in the S mode, in the F mode *net* reaches a maximal value of only 60–70% in the voltage range between −40 mV and 0 mV. A reason for this difference might be a substantial degree of closed-channel inactivation in the F mode. This could be the result of a faster closed-channel inactivation in the F mode ($\gamma_F \gg \delta_{S,P}$) in competition with an activation process similar to that in the S mode ($\alpha_{F,S}$). Unfortunately, due to the short mean open time in the F mode, there should be significantly more missed openings compared with the S mode. Therefore, it is diffi-

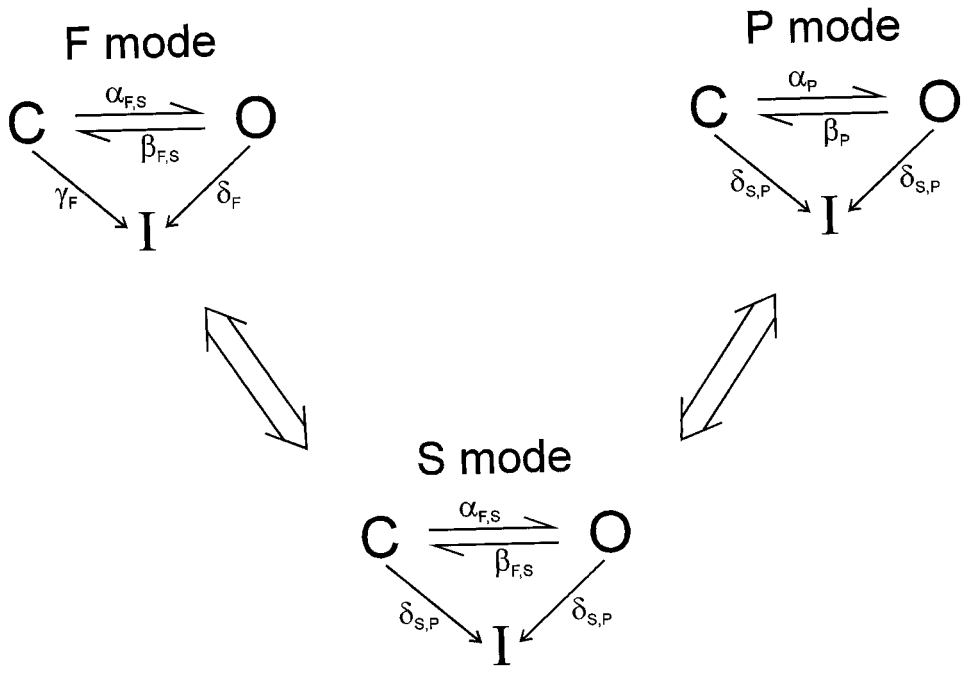

FIGURE 10 State model for the F, S, and P modes. Each of the three modes is represented by a single closed (C), open (O), and inactivated state (I). The latter is assumed to be absorbing. The rate constants for activation ($\alpha_{F,S}$) and deactivation ($\beta_{F,S}$) are the same in the F and S modes but differ from those in the P mode (α_P and β_P). The rate constants for open- and closed-channel inactivation are identical in the S and P modes ($\delta_{S,P}$) but differ from those in the F mode (δ_F and γ_F).

cult to estimate the amount of closed-channel inactivation in the F mode.

In the S mode, the observed 10% empty traces in the voltage range between −60 mV and 0 mV cannot be attributed to missed openings because of the long mean open times. Two interpretations for the observation of an empty trace seem to be reasonable. 1) The channel may not be available at the beginning of the pulse protocol. 2) The channel inactivates without opening. The latter interpretation seems to be very unlikely, because *net* is constant at 90% over a wide voltage range. Then closed-channel inactivation and channel activation would be voltage dependent to the same degree, because these processes are always in competition. Therefore, we prefer the interpretation that the channel is not available in 10% of the traces. A possible reason might be that at the holding potential, recovery from inactivation is slow compared with the pulsing frequency. For further analysis, recovery from inactivation should be studied.

In comparison with the S mode, in the P mode, there is a larger amount of empty traces at all voltages. The maximal value of *net* in the P mode is 80% at +20 mV. At this voltage, the large number of empty traces cannot be caused by missed events. The difference may be attributed to the slower activation kinetics of the P mode compared with the S mode, with the consequence of a more probable closed-channel inactivation (compare τ_h and first latency).

Macroscopic inactivation kinetics can be interpreted in the following way. In the F mode, the time constant of macroscopic inactivation (τ_h) seems to be determined mainly by the latency until the first channel opening (Böhle and Benndorf, 1995b). Both open- and closed-channel inactivation are presumably faster. Conversely, in the S and P modes, τ_h is supposed to be mainly determined by the number of reopenings and subsequent microscopic inactivation ($\delta_{S,P}$). In the S mode, mainly open channels inactivate (cessation of prolongation of the mean open-channel lifetime (τ_o) positive to −40 mV; Böhle and Benndorf, 1995b). In the P mode, reclosing dominates over open-channel inactivation, and mainly closed channels inactivate (prolongation of τ_o up to 0 mV; Böhle and Benndorf, 1995b).

It may be concluded that the model presented in Fig. 10 is a useful scheme for functional interpretation of mode switching. Future experiments on the onset of and restoration from inactivation might help to develop a more detailed model.

Possible implications of gating modes

When considering possibilities for the physiological or pathophysiological role of the individual gating modes, major limitations arise from the missing knowledge about both the dwell times in each mode and the mechanisms triggering the mode switching. As in multiple other excitable cells, the cardinal function of the Na^+ current in cardiac ventricular cells is to mediate the rapid depolarization phase of the action potential (phase 0). This rapid depolarization phase is a prerequisite for an effective con-

traction of the heart muscle. It may be speculated that the coexistence of Na^+ channels in multiple gating modes is an inherent property of these molecules. Alternatively, the cells may also adapt their modes to the actual requirements with respect to the surrounding cells, e.g., to suppress arrhythmias. In this sense, switching to the S mode should accelerate the depolarizing phase, whereas switching to the P mode would cause the opposite effect.

Cardiac Na^+ current has also been identified to prolong the action potential duration (Coraboeuf et al., 1979; Carmeliet, 1987). The easiest explanation of this finding is that a small minority of Na^+ channels loses inactivation and stays open for several hundreds of milliseconds, e.g., by switching to non-inactivating modes (Patlak and Ortiz, 1985), which may also be provoked by a variety of drugs (Nilius et al., 1989; Kohlhardt et al., 1987). At variance to these findings, all modes discussed in the present report inactivate too rapidly to expect any influence on the action potential duration of the human ventricular myocardium. One has to be aware, however, that the action potential of mouse ventricular myocytes is extremely short (2–3 ms at 50% repolarization; Doepner et al., 1997). The open-probability of even the F mode may be relatively large during such a short action potential. In these cells, it is likely that the S and P modes indeed contribute to the control of the action potential duration. With the knowledge of more slowly inactivating gating modes in heart cells with significantly longer action potentials (Patlak and Ortiz, 1985; Liu et al., 1992; Mazzanti and DeFelice, 1987), one may further speculate that inactivation kinetics of slower gating modes is proportional to the action potential duration; i.e., cells with long action potentials would generate gating modes with slower inactivation kinetics than cells with short action potentials. The practical implication of altered inactivation in Na^+ channels is found in certain diseases and has recently been discussed by Cannon (1996). Several inherited myopathies have been mapped to the human skeletal muscle Na^+ channel gene (Stephan and Agnew, 1991; Barchi, 1995), for example, paramyotonia congenita and hyperkalemic periodic paralysis (HyperPP). Cummins et al. (1993) investigated the respective point mutation in the rat skeletal muscle Na^+ channel (rT698M) causing HyperPP and found a negative shift of the steady-state activation curve. This increases the amount of overlap between steady-state activation and inactivation and results in window current, which can be important in HyperPP pathophysiology. Cummins and Sigworth (1996) came to the conclusion that in the rT698M channels, both activation and slow inactivation was modified.

Similar to Na^+ channels in other tissues, also in cardiac Na^+ channels (hH1), bursts have been observed (Gellens et al., 1992), which may reflect distinct gating modes. Recently, it has been suggested (Bennett et al., 1995) that one form of an inherited cardiac arrhythmia disease, named congenital long-QT syndrome (LQT3), is caused by a point mutation in the hH1 Na^+ channel gene. Functional expression of these Na^+ channels showed that the fluctuation between normal and non-inactivating gating modes was affected such that late openings occurred more often.

We thank D. Metzler, R. Kemkes, K. Schoknecht, B. Tietsch, and A. Kolchmeier for excellent technical assistance.

REFERENCES

Attwell, D., I. Cohen, D. Eisner, M. Ohba, and C. Ojeda. 1979. The steady-state TTX-sensitive ("window") Na current in cardiac Purkinje fibers. *Pflügers Arch.* 379:137–142.

Barchi, R. L. 1995. Molecular pathology of the skeletal muscle sodium channel. *Annu. Rev. Physiol.* 57:355–385.

Benndorf, K. 1993. Multiple levels of native cardiac Na^+ channels at elevated temperature measured with high-bandwidth/low-noise patch clamp. *Pflügers Arch.* 422:506–515.

Benndorf, K. 1995. Low noise recording. *In* Single Channel Recording, 2nd ed. B. Sakmann and E. Neher, editors. Plenum Press, New York. 129–145.

Bennett, P. B., K. Yazawa, N. Makita, and A. L. George Jr. 1995. Molecular mechanism for an inherited cardiac arrhythmia. *Nature.* 376: 683–685.

Böhle, T., and K. Benndorf. 1994. Facilitated giga-seal formation with a just originated glass surface. *Pflügers Arch.* 427:487–491.

Böhle, T., and K. Benndorf. 1995a. Multimodal action of single Na^+ channels in myocardial mouse cells. *Biophys. J.* 68:121–130.

Böhle, T., and K. Benndorf. 1995b. Voltage-dependent properties of three different gating modes in single cardiac Na^+ channels. *Biophys. J.* 69:873–882.

Brown, K. M., and J. E. Dennis. 1972. Derivative-free analogues of the Levenberg-Marquardt and Gauss algorithms for nonlinear least squares approximation. *Num. Math.* 18:289–297.

Cannon, S. C. 1996. Slow inactivation of sodium channels: more than just a laboratory curiosity. *Biophys. J.* 71:5–7.

Carmeliet, E. 1987. Slow inactivation of the sodium current in rabbit cardiac Purkinje fibres. *Pflügers Arch.* 408:18–26.

Chandler, W. K., and H. Meves. 1970. Evidence for two types of sodium conductances in axons perfused with sodium fluoride solution. *J. Physiol.* 211:653–678.

Coraboeuf, E., E. Deroubaix, and A. Coulombe. 1979. Effect of tetrodotoxin on action potentials of the conducting system in the dog heart. Am. J. Physiol. 236:H561–H567.

Correa, A. M., and F. Bezanilla. 1994. Gating of the squid sodium channel at positive potentials. II. Single channels reveal two open states. *Biophys. J.* 66:1864–1878.

Cummins, T. R., and F. J. Sigworth. 1996. Impaired slow inactivation in mutant sodium channels. *Biophys. J.* 71:227–236.

Cummins, T. R., J. Zhou, F. J. Sigworth, C. Ukomadu, M. Stephan, L. J. Ptacek, and W. S. Agnew. 1993. Functional consequences of a Na^+ channel mutation causing hyperkalemic periodic paralysis. *Neuron.* 10: 667–668.

Doepner, B., S. Thierfelder, H. Hirche, and K. Benndorf. 1997. 3-Hydoxybutyrate blocks the transient K^+ outward current in myocardial mouse cells in a stereoselective fashion. *J. Physiol.* 500.1:85–94.

Gellens, M. E., A. L. George Jr., L. Chen, M. Chahine, R. Horn, R. L. Barchi, and R. G. Kallen. 1992. Primary structure and functional expression of the human cardiac tetrodotoxin-insensitive voltage-dependent sodium channel. *Proc. Natl. Acad. Sci. USA.* 89:554–558.

Gilly, W. M. F., and C. M. Armstrong. 1984. Threshold channels: a novel type of sodium channel in squid giant axon. *Nature.* 309:448–450.

Grant, A. O., and C. F. Starmer. 1987. Mechanism of closure of cardiac sodium channels in rabbit ventricular myocytes: single-channel analysis. *Circ. Res.* 60:897–913.

Keynes, R. D. 1994. Bimodal gating of the Na^+ channel. *Trends Neurosci.* 17:58–61.

Keynes, R. D., and H. Meves. 1993. Properties of the voltage sensor for the opening and closing of the sodium channels in the squid giant axon. *Proc. R. Soc. Lond. B.* 253:61–68.

Kohlhardt, M., U. Fröbe, and J. W. Herzig. 1987. Properties of normal and non-inactivating single cardiac Na^+ channels. *Proc. R. Soc. Lond. B.* 232:71–93.

Liu, Y., L. J. DeFelice, and M. Mazzanti. 1992. Na channels that remain open throughout the cardiac action potential plateau. *Biophys. J.* 63: 654–662.

Mazzanti, M., and L. J. DeFelice. 1987. Na channel kinetics during the spontaneous heart beat in chick ventricle cells. *Biophys. J.* 52:95–100.

Mitsuiye, T., and A. Noma. 1995. Inactivation of the cardiac Na^+ channels in guinea-pig ventricular cells through the open state. *J. Physiol.* 485: 581–594.

Nilius, B., J. Vereecke, and E. Carmeliet. 1989. Properties of the bursting Na channel in the presence of DPI 201–106 in guinea-pig ventricular myocytes. *Pflügers Arch.* 413:234–241.

Patlak, J. B. 1988. Sodium channel subconductance levels measured with a new variance-mean analysis. *J. Gen. Physiol.* 92:413–430.

Patlak, J. B., and M. Ortiz. 1985. Slow currents through single sodium channels of the adult rat heart. *J. Gen. Physiol.* 86:89–104.

Saint, D. A., Y. K. Ju, and P. W. Gage. 1992. A persistent sodium current in rat ventricular myocytes. *J. Physiol.* 453:219–231.

Stephan, M., and W. S. Agnew. 1991. Voltage-sensitive Na^+ channels: motifs, modes, and modulation. *Curr. Opin. Cell. Biol.* 3:676–684.

Yue D. T., J. H. Lawrence, and E. Marban. 1989. Two molecular transitions influence cardiac sodium channel gating. *Science.* 244:349–352.

Zilberter, Y. I., and L. G. Motin. 1991. Existence of two fast inactivation states in cardiac Na^+ channels confirmed by two-stage action of proteolytic enzymes. *Biochim. Biophys. Acta.* 1068:77–80.